Tuijin Jishu/Journal of Propulsion Technology
ISSN: 1001-4055
Vol. 44 No. 5 (2023)

Heat Gneration on Three Dimensional Casson Nanofluid Motion with Arrhenius Activation Energy Effect Via Stretching Sheet

Adilakshmi Velivela1[*], G. Venkata Ramana Reddy[2]

[1*]*Research Scholar, Department of Mathematics, Koneru Lakshmaiah Education Foundation, Vaddeswaram, Andrapradesh-522302, India*

[2]*Department of Mathematics, Professor, Koneru Lakshmaiah Education Foundation, Vaddeswaram, Andrapradesh-522302, India*

Abstract: **-** The current study Arrhenius activation energy effect on 3D porous Casson nanofluid (NFs) motion via stretching sheet (SS) is explored in this study using numerical process based on Runge Kutta Fehlberg (R-K-F). To provide useful visions into the physical and dynamic examinations of this study, convective heat and mass boundary conditions are used. The established of nonlinear partial differential equations (PDEs) has been transported into ordinary differential equations (ODEs) by helping suitable similarity transformations. The translated ODEs are computed by help of shooting iterative approach. The outcomes of this study are validated with previous investigations, and get excellent agreements. The behaviour of different physical parameters is analysed. It is observed that, the heat transfer rate is high in presence of Activation energy for large values Prandtl number and mass transfer rate decline low in presence of Activation energy for numerical values of Lewis number.

Keywords*: Arrhenius Activation Energy, Casson nanaofluid, Heat Source.*

1. Introduction

The study of nanofluids has drawn a lot of interest in the field of fluid mechanics and heat transfer, primarily owing to their unique thermal characteristics and potential usage in various engineering and industrial processes. Alwawi et al. [1] exhibited steady laminar two-dimensional incompressible MHD Casson nanofluid motion via solid sphere. Archana et al. [2] presented Casson nanofluid motion between two parallel plates. Shah et al. [3] developed entropy optimization on Casson nanofluid flowing via stretchable nonlinear surface. Jamshed et al. [4] examined the Casson nanofluid motion with convection slip conditions in presence of thermal transformation. Akaje and Olajuwon [5] presented the impact of nonlinear radiative on species heat transfer while taking Thompson and Troian boundary conditions. Obalalu et al. [6] concentrated the second-order velocity slip and heat transfer caused by nanofluid along with non-Darcian Casson flow via permeable stretching surface. Satya Narayana et al. [7] investigated the couple stress Casson fluid flow via internally heated and horizontally stretched surface. Dahab et al. [8] studied the viscoelastic fluid flow via nonlinearly stretched surface. Sahoo and Nandkeolyar [9] examined the entropy production in a three-dimensional Casson nanofluid motion. Akinshilo et al. [10] exhibited non-Newtonian Casson nanofluid motion around a small needle. Mahanta et al. [11] focused on the real-world uses of nanoparticles in non-Newtonian base fluids with energy conversion and heat generation.

Casson nanofluid is a novel and fascinating class of complex fluids that has attracted considerable interest recently due to its exceptional rheological characteristics and potential use in a wide range of engineering and scientific fields. This special nanofluid combines the properties of yield stress-behaving Casson fluids with the improved heat transfer capabilities provided by the incorporation of nanoparticles. Wang et al. [12] examined the three-dimensional motion of couple stress Casson liquid. Tarakaramu et al. [13] analyzed the 3D nanofluid motion with convective conditions via stretching sheet. Waqas et al. [14] presented the Falkner-Skan bioconvection flow of a

cross nanofluid motion via moving wedge. Khan et al. [15] studied the movement of heat and mass in an Oldroyd-B fluid motion via rotating disk. Shankar Goud et al. [16] focused MHD Casson fluid flow via non-linear inclined stretching surface with velocity slip. Riaz Khan et al. [17] concentred the stagnation point motion of a time-dependent Casson fluid via permeable stretching/shrinking surface. Jalili et al. [18] have studied the effect of nonlinear thermal radiation on non-Newtonian fluids motion various flow geometries. Abbas et al. [19] focused unsteady compressible Casson hybrid nanofluid motion via vertically stretching sheet. Rana et al. [20] examined heat transport and nonlinear thermal buoyancy-driven flow in a hybrid nanofluid (MWCNT-MgO/EG) at a rotating sphere's stagnation point. Bhagya Lakshmi et al. [21] Investigated the convective heat and mass transfer in the context of magnetohydrodynamic flow of a Casson fluid over a curved surface. Narsu Sivakumar et al. [22] revealed that the Casson fluid's rate of heat transfer increases as the magnetic field intensity increases, but beyond a certain threshold, this relationship changes, resulting in a drop in the heat transfer rate. Asifa et al. [23] Examined the non-uniform velocity, magnetohydrodynamics, and Newtonian heating-influenced unsteady flow of a rate-type fluid close to a vertical plate. Using the fractional operators, three distinct fractional models for the fluid's behaviour are investigated. Tarakaramu et al [24] Investigated heat and mass transfer in a three-dimensional couple stress Casson fluid flow with nonlinear thermal radiation and heat source effects. Some of authors [25-27] developed three dimensional nanofluid motion via stretching sheet.

2. Mathematical Analysis:

Consider 3D magnetohydrodynamic flow of a non-Newtonian nanofluid over a stretching sheet $z^* = 0$ along $x^*\ y^*$-plane while fluid is located along with z^*-direction. The fluid flow region is taken as $z > 0$. The velocity components $u_1 = a^* x^*$ and $u_2 = b^* y^*$ along $x^*\ y^*$- directions respectively as shown in **Fig. 1**. Moreover, it has taken that the constant Magnetic field is applied normal to the fluid flow direction and it is assumed that induced magnetic field is negligible. We considered that the rheological equation of extra stress tensor τ for an isotropic and incompressible flow of a Casson fluid can be written as. Usually, Casson model is used as a constitutive equation of blood. But in this study, viscosity model is used as a constitute equation of blood. This model is written as:

$$\tau_{ij} = \begin{cases} 2e_{ij}\left(\mu_B^* + p_y \big/ \sqrt{2\Pi}\right), & \Pi > \Pi_c \\ 2e_{ij}\left(\mu_B^* + p_y \big/ \sqrt{2\Pi_c}\right), & \Pi < \Pi_c \end{cases}$$

Based on above construction we have to formulate the governing equations in the present flow analysis as:

$$\frac{\partial u_1}{\partial x^*} + \frac{\partial u_2}{\partial y^*} + \frac{\partial u_3}{\partial z^*} = 0 \tag{1}$$

$$u_1\frac{\partial u_1}{\partial x^*} + u_2\frac{\partial u_1}{\partial y^*} + u_3\frac{\partial u_1}{\partial z^*} = \upsilon^*\left(1+\frac{1}{\beta}\right)\frac{\partial^2 u_1}{\partial z^{*2}} - \frac{\sigma^* B_0^2}{\rho^*}u_1 \tag{2}$$

$$u_1\frac{\partial u_2}{\partial x^*} + u_2\frac{\partial u_2}{\partial y^*} + u_3\frac{\partial u_2}{\partial z^*} = \upsilon^*\left(1+\frac{1}{\beta}\right)\frac{\partial^2 u_2}{\partial z^{*2}} - \frac{\sigma^* B_0^2}{\rho^*}u_2 \tag{3}$$

$$u_1\frac{\partial T^*}{\partial x^*} + u_2\frac{\partial T^*}{\partial y^*} + u_3\frac{\partial T^*}{\partial z^*} = \alpha_m\frac{\partial^2 T^*}{\partial z^{*2}} - \frac{1}{(\rho^* C^*)_f}\frac{\partial q_r}{\partial z^*} - \frac{Q_0}{(\rho^* C^*)_f}(\mathrm{T}^* - \mathrm{T}_\infty^*) + \varsigma_1\left(D_B\frac{\partial T^*}{\partial z^*}\frac{\partial C^*}{\partial z^*} + \frac{D_T}{T_\infty^*}\left(\frac{\partial T^*}{\partial z^*}\right)^2\right) \tag{4}$$

$$u_1\frac{\partial C^*}{\partial x^*} + u_2\frac{\partial C^*}{\partial y^*} + u_3\frac{\partial C^*}{\partial z^*} = \left(D_B\frac{\partial^2 C^*}{\partial\left(z^*\right)^2} + D_T \big/ T_\infty^*\frac{\partial^2 T^*}{\partial\left(z^*\right)^2}\right) - K_r^2\left(C^* - C_\infty^*\right)\left(\frac{T^*}{T_\infty^*}\right)^m \exp\left(\frac{-E_1 a_1}{k_1 T^*}\right) \tag{5}$$

The relevant boundary conditions of the present model as

$$\left.\begin{array}{l} u_1 = a^* x^*, \quad u_2 = b^* y^*, \quad u_3 = 0, \quad -k^* \dfrac{\partial T^*}{\partial z^*} = h^* (\mathrm{T}_f^* - \mathrm{T}^*), \quad -D\left(\dfrac{\partial C^*}{\partial z^*}\right) = h^* \left(C_f^* - C^*\right) \text{ at } u_3 = 0 \\ u_1 \to 0, \quad u_2 \to 0, \quad T^* \to T_\infty^*, \quad C^* \to C_\infty^* \quad \text{as} \quad u_3 \to \infty \end{array}\right\} \tag{6}$$

The radiative heat flux q_r which is given by Quinn Brewster **[28]** is given by

$$q_r = -\frac{4\sigma^*}{3K^*}\frac{\partial T^{*4}}{\partial z^*} = -\frac{16\sigma^*}{3K^*} T^{*3} \frac{\partial T^*}{\partial z^*} \Bigg\} \tag{7}$$

Differentiate above heat flux equation, we get

$$\frac{\partial q_r}{\partial z^*} = -\frac{16\sigma^*}{3K^*}\frac{\partial}{\partial z^*}\left(T^3 \frac{\partial T^*}{\partial z^*}\right) \tag{8}$$

Substituting **Eq. (8)** in **Eq. (4),** we get below Expression

$$\left.\begin{array}{l} u_1 \dfrac{\partial T^*}{\partial x^*} + u_2 \dfrac{\partial T^*}{\partial y^*} + u_3 \dfrac{\partial T^*}{\partial z^*} = \alpha_m \dfrac{\partial^2 T^*}{\partial z^{*2}} + \dfrac{1}{(\rho^* C^*)_f}\left(\dfrac{16\sigma^*}{3K^*}\dfrac{\partial}{\partial z^*}\left(T^{*3}\dfrac{\partial T^*}{\partial z^*}\right)\right) - \dfrac{Q_0}{(\rho^* C^*)_f}(\mathrm{T}^* - \mathrm{T}_\infty^*) \\ \qquad + \dfrac{(\rho^* C^*)_p}{(\rho^* C^*)_f}\left(D_B \dfrac{\partial T^*}{\partial z^*}\dfrac{\partial C^*}{\partial z^*} + \dfrac{D_T}{T_\infty^*}\left(\dfrac{\partial T^*}{\partial z^*}\right)^2\right) \end{array}\right\} \tag{9}$$

The similarity transformations as below

$$\left.\begin{array}{l} \eta_1 = \sqrt{\dfrac{a^*}{\upsilon^*}}\, z, \quad u_1 = a^* x^* f'(\eta_1), \quad u_2 = a^* y^* g'(\eta), \quad u_3 = -\sqrt{a^* \upsilon^*}\,(f(\eta_1) + g(\eta_1)) \\ \theta(\eta_1) = \dfrac{T^* - T_\infty^*}{T_w^* - T_\infty^*}, \quad \phi(\eta) = \dfrac{C^* - C_\infty^*}{C_w^* - C_\infty^*} \end{array}\right\} \tag{10}$$

Using above **Eq. (10)**, we are converting **Eq. (2)-(4)** and **Eq. (9)** into below format

$$f'''\left(1 + \frac{1}{\beta}\right) + f''(f + \mathrm{g}) - (f')^2 - Mf' = 0 \tag{11}$$

$$\mathrm{g}'''\left(1 + \frac{1}{\beta}\right) + g''(f + \mathrm{g}) - (g)^2 - Mg' = 0 \tag{12}$$

$$\left(\left(1 + R_d(\theta(\theta_w - 1) + 1)^3\right)\theta'\right)' + \mathrm{Pr}\left((f + \mathrm{g})\theta' + N_b \theta'\phi' + \mathrm{N}_t\, \theta'^2\right) + H\theta = 0 \tag{13}$$

$$\phi'' + Le(f + \mathrm{g})\phi' + \frac{N_t}{N_b}\theta'' - LeD(1 + R\theta)^r\, e^{\left(-E/1+R\theta\right)} = 0 \tag{14}$$

Corresponding boundary conditions as below

$$\left.\begin{array}{l} f = 0, \quad g = 0, \quad f' = 1, \quad g' = \lambda, \quad \theta' = -Bi_t(1 - \theta), \quad \phi' = -Bi_c(1 - \phi()) \ \ at \ \eta_1 = 0 \\ f' \to 0, \quad g' \to 0, \quad \theta \to 0, \quad \phi \to 0, \quad \text{as} \ \ \eta_1 \to \infty \end{array}\right\} \tag{15}$$

Moreover, the skin-friction coefficient and Nusselt number are below

$$\left.\begin{array}{l} \left(\mathrm{Re}_x\right)^{1/2} C_{fx} = \left(1 + \dfrac{1}{\beta}\right) f''(0), \qquad \left(\mathrm{Re}_x\right)^{1/2} C_{fy} = \left(1 + \dfrac{1}{\beta}\right)\mathrm{g}''(0) \\ \left(\mathrm{Re}_x\right)^{-1/2} Nu_x = -\left(1 + R_d(\theta(\theta_w - 1) + 1)^3\right)\theta'(0), \quad \mathrm{ShRe}_x^{-1/2} = -\phi'(0) \end{array}\right\} \tag{16}$$

3. Results and Discussion

The characteristics of β (Casson parameter) on $\mathrm{g}'(\eta)$ ("Transverse Direction) as shown in **Fig. 2**. The velocity of Casson nanofluid motion decrease on $\mathrm{g}'(\eta)$ ("Transverse Direction"). Physically, the Casson parameter is proportional to dynamic viscosity, due to this the low viscosity in Casson liquid motion reduces velocity of liquid at stretching surface.

The most significant effects Pr (Prandtl Number), H (Heat Generation Parameter), R_d (nonlinear thermal radiation) on $\theta(\eta_1)$ with the cases of presence and absence of Casson fluid as presented in **Figs. 3(a)-3(b),** respectively. It is perceived that the fluid temperature declined more in presence of Casson liquid while compared with absence of Casson liquid with distinct numerical values of Pr, H while opposite direction of liquid temperature moves for large numerical values of R_d. Physically, the Prandtl number is relation between to thermal conductivity and thermal diffusivity, due to this the high thermal diffusivity of Casson nanofluid released low temperature and also low absorption of liquid motion produces high temperature.

The most significant effects Pr (Prandtl Number) on $Nu_x \, \mathrm{Re}_x^{-0.5}$ with the cases of presence and absence of Activation energy as shown in **Figs. 4**. It is perceived that the heat transfer enhanced in more when presence of activation energy while compared with absence of activation energy with distinct numerical values of Pr. We conclude that, the present study developed more heat transfer when presence of Activation energy in Casson nanofluid motion at stretching surface.

The variation of θ_w (Temperature Ratio Parameter), N_b (Brownian Motion Parameter) and N_t (Thermophoresis Parameter) on $\theta(\eta_1)$ with the cases of Presence and absence of Casson liquid and heat generation effect as predicted in **Figs. 5(a)-5(c)**. It is perceived that the temperature of Casson nanofluid motion for the presence of activation energy when compared to absence of activation energy. Physically, the Brownian diffusivity and thermal diffusivity applied into Casson nanofluid motion, in that the base fluid particles crashed between each other and then produces more temperature at stretching surface.

The variation of Le (Lewies number) on $Sh_x \, \mathrm{Re}_x^{-1.5}$ with the cases of presence and absence of activation energy liquid has displayed in **Fig. 6.** It is noticed that the mass transfer rate reduction low for presence of activation energy while compared to absence of activation energy with raising values of Le. Physically, Brownian diffusivity reduces mass transfer of Casson nanofluid motion at surface area.

4. Conclusion

The main outcomes of current study as presented in below:

- The temperature of Casson nanofluid is high in presence of Activation energy and heat generation effects for enhanced numerical values of R_d, N_b, N_t.
- The heat transfer rate is high in presence of Activation energy for large numerical values of Prandtl number.
- The mass transfer rate if very low in presence of Activation energy while compared with absence f activation energy for large numerical values of Lewis number.

Refrences

[1] A.F. Alwawi, T.H. Alkasasbeh, A.M. Rashad and I. Ruwaidiah, MHD natural convection of Sodium Alginate Casson nanofluid over a solid sphere, Result in Physics, 16 (2020) 102818. https://doi.org/10.1016/j.rinp.2019.102818.

[2] M. Archana, M.M. Praveena, K. Ganesh Kumar, S.A. Shehzad and M. Ahmad, Unsteady squeezed Casson nanofluid flow by considering the slip condition and time-dependent magnetic field, Heat Transfer, 49(8) (2020) 4907-4922. DOI: 10.1002/htj.21859.

[3] Z. Shah, P. Kumam and W. Deebani, Radiative MHD Casson Nanofluid Flow with Activation energy and chemical reaction over past nonlinearly stretching surface through Entropy generation, Scientific Reports, 10 (2020) 4402. https://doI.or g/10.038/s41598-020-61125-9.

[4] W. Jamshed, S.S. Uma Devi, M. Goodarzi, M. Prakash, K. Sooppy Nisar and M. Zakarya, and A.A. Abdel-Haleem, Evaluating the unsteady Casson nanofluid over a stretching sheet with solar thermal radiation: An optimal case study, Case Studies in Thermal Engineering, 26 (2021) 101160. https://doi.org/10.10 16/j.csite.2021.1011 6.0.

[5] T.W. Akaje and B.I. Olajuwon, Impacts of Nonlinear Thermal Radiation on a Stagnation Point of an Aligned MHD Casson Nanofluid Flow with Thompson and Troian Slip Boundary Condition, Journal of Advanced Research in Experimental Fluid Mechanics and Heat Transfer, 6(1) (2021) 1-15.

[6] A.M. Obalalu, O.A. Ajala, A. Abdulraheem and A.O. Akindele, The influence of variable electrical conductivity on non-Darcian Casson nanofluid flow with first and second-order slip conditions, Partial Differential Equations in Applied Mathematics, 4 (2021) 100084. Https://doi.org /10.1016/j.pad iff.2021.100084.

[7] P.V. Satya Narayana, N. Tarakaramu, G. Sarojamma, I.L. Animasaun, Numerical Simulation of Nonlinear Thermal Radiation on the 3D Flow of a Couple Stress Casson Nanofluid Due to a Stretching Sheet, Journal of Thermal Science and Engineering, 13(2) (2021) 021028. https://doi.org/10.1115/1.4049425.

[8] S.M.A. Dahab, M.A. Abdelhafez, F. Mebarek Oudina and S.M. Bilal, MHD Casson nanofluid flow over nonlinearly heated porous medium in presence of extending surface effect with suction/injection, Indian Journal of Physics, 95 (2021) 2703-2717. Https://doi.org/ 10.1007/s12648-020-01923-z.

[9] A. Sahoo and R. Nandkeolyar, Entropy generation and dissipative heat transfer analysis of mixed convective hydromagnetic flow of a Casson nanofluid with thermal radiation and Hall current, Science Direct, 11 (2021) 3926. https://doi.org/10.1038/s 41598-02183124-0.

[10] A.T. Akinshilo, F. Mabood and A.O. Ilegbusi, Heat generation and nonlinear radiation effects on MHD Casson nanofluids over a thin needle embedded in porous medium, International Communications in Heat and Mass Transfer, 127 (2021) 105547. https://doi.org/10.1016/j.icheatmasstransfer.2021.105547.

[11] G. Mahanta, M. Das, M.K. Nayak, and S. Shaw, Irreversibility Analysis of 3D Magnetohydrodynamic Casson Nanofluid Flow Past Through Two Bi-Directional Stretching Surfaces with Nonlinear Radiation, Journal of Nanofluids, 10(3) (2021) 316-326(11). doi:10.1166/jon.2021.1793.

[12] F. Wang, N. Tarakaramu, N. Sivakumar, P.V. Satya Narayana, D. Harish Babu, SR. Sivajothi, Three dimensional nanofluid motion with convective boundary condition in presents of nonlinear thermal radiation via stretching sheet, Journal of the Indian Chemical Society, 100(2) (2023) 100557. http://dx.doi.org/10.1016/ j. jics.2023.100887.

[13] N. Tarakaramu, P.V. Satya Narayana, R. Sivajothi, K. Bhagya Lakshmi, D. Harish Babu and B. Venkateswarlu, Three-dimensional non-Newtonian couple stress fluid flow over a permeable stretching surface with nonlinear thermal radiation and heat source effects, Heat Transfer, 51(6) (2021) 5348-5367. DOI: 10.1002/htj.22550.

[14] H. Waqas, S.A. Khan, S.U. Khan, M. Ijaz Khan, S. Kadry and Y. Ming Chu, Falkner-Skan time-dependent bioconvection flow of cross nanofluid with nonlinear thermal radiation, activation energy and melting process, International Communications in Heat and Mass Transfer, 120 (2021) 105028. Https://doI.org/10.1016 /j.Icheatmasstrans fer.2020.105028

[15] M. Khan, A. Hafeez and J. Ahmed, Impacts of non-linear radiation and activation energy on the axisymmetric rotating flow of Oldroyd-B fluid, Physica A: Statistical Mechanics and its Applications, 580 (2021) 124085. https://doI.org/10 .1016/j.physa .2019. 124085.

[16] B. Shankar Goud, Y. Dharmendar Reddy, W. Jamshed, K. Sooppy Nisar, N. A. Alharbi and R. Chouikh, Radiation effect on MHD Casson fluid flow over an inclined non-linear surface with chemical reaction in a Forchheimer porous medium, Alexandria Engineering Journal, 61(10) (2022) 8207-8220. https://doI.org /10.1016/j.aej.2022.01.043.

[17] M. Riaz Khan, A.S.A. Johani, A.M.A. Elsiddieg, T. Saeed and A.A.A. Mousa, The computational study of heat transfer and friction drag in an unsteady MHD radiated Casson fluid flow across a stretching/shrinking surface, International Communications in Heat and Mass Transfer, 130 (2022) 105832. Https:/doi.org/101016/j. icheatmasstransfer.2021.105832.

[18] P. Jalili, A.A. Azar, B. Jalili, D.D. Ganji, Study of nonlinear radiative heat transfer with magnetic field for non-Newtonian Casson fluid flow in a porous medium, Result in Physics, 48 (2023) 106371. https://doi.org/10.1016/j.rinp .2023 .1063 71.

[19] N. Abbas, W. Shatanawi and K. Abodayeh, Computational Analysis of MHD Nonlinear Radiation Casson Hybrid Nanofluid Flow at Vertical Stretching Sheet, Symmetry, 14(7) (2022) 1494. https://doi.org/10.3390/sym14071494.

[20] P. Rana, S. Gupta and G. Gupta, Unsteady nonlinear thermal convection flow of MWCNT-MgO/EG hybrid nanofluid in the stagnation-point region of a rotating sphere with quadratic thermal radiation: RSM for optimization, International Communications in Heat and Mass Transfer, 134 (2022) 106025. https://doI.org/10.1016 /j. icheatmasstransfer.2022.106025.

[21] K. Bhagya Lakshmi, V. Sugunamma, N. Tarakaramu and N. Sivakumar R. Sivajothi, Cross-dispersion effect on magnetohydrodynamic dissipative Casson fluid flow via curved sheet, Heat Transfer, 51(8) (2022) 7822-7842. DOI: 10.1002/htj.22668.

[22] N. Sivakumar, N. Tarakaramu, P.V. Satya Narayan, K. Bhagya Lakshmi and B. Aruna Kumari, Three dimensional magnetohydrodynamic Casson fluid flow over a linear stretching surface: A numerical analysis, AIP Conference Proceedings, 2516 (2022) 170022, DOI: 10.1063/5.0110704.

[23] Asifa, P. Kumam, A. Tassaddiq, W. Watthayu, Z. Shah and T. Anwar, Modeling and simulation-based investigation of unsteady MHD radiative flow of rate type fluid; a comparative fractional analysis, Mathematics and Computers in Simulation, 201 (2022) 486-507. https://doi.org/10.1016/j.matcom.2021.02.005.

[24] N. Tarakaramu, P.V. Satya Narayana, N. Sivakumar, D. Harish Babu and K. Bhagya Lakshmi, Convective Conditions on 3D Magnetohydrodynamic (MHD) Non-Newtonian Nanofluid Flow with Nonlinear Thermal Radiation and Heat Absorption: A Numerical Analysis, Journal of Nanofluids, 12(2) (2023) 448-457(10). http://dx.doI.org/10 .1166/jon.2023.1939.

[25] N. Tarakaramu, N. Sivakumar, N. Tamam, P. V. Satya Narayana, S. Ramalingam, Theoretical analysis of Arrhenius activation energy on 3D MHD nanofluid flow with convective boundary condition, Modern Physics Latters B, (2023) 2341009.

[26] G. Radha, B. Reddappa, N. Tarakaramu, V.K. Somasekhar Srinivas, R. Sivajothi, N. Mallikarjuna Reddy, K. Amaranadha Reddy, K. Bhagya Lakshmi, Three Dimensional Casson nanofluid Flow with Convective Boundary Layer via Stretching Sheet, Journal of Advanced Zoology, 44(S-5) 1121-1129.

[27] M. Revathi Devi, N. Sivakumar, N. Tarakaramu, P.V. Satya Narayana, The impact of heat source and thermal radiation on nano-bioconvection containing gyrotactic microorganism flow in parallel channel, AIP Conference Proceedings, 2852 (2023) 050010.

[28] M. Q. Brewster, Thermal radiative transfer properties, Wiley, New York, 1972.

[29] C. Y. Wang, The three-dimensional flow due to a stretching flat surface, Phys. Fluids 27 (1915) (1984) 1-4. Doi: 10.1063/1.864868.

[30] G.T. Thammanna, K. Ganesh Kumar, B.J. Gireesha, G.K. Ramesh and B.C. Prasannakumara, three dimensional MHD flow of couple stress Casson fluid past an unsteady stretching surface with chemical reaction, Results Physics, 7 (2017) 4104-4110.

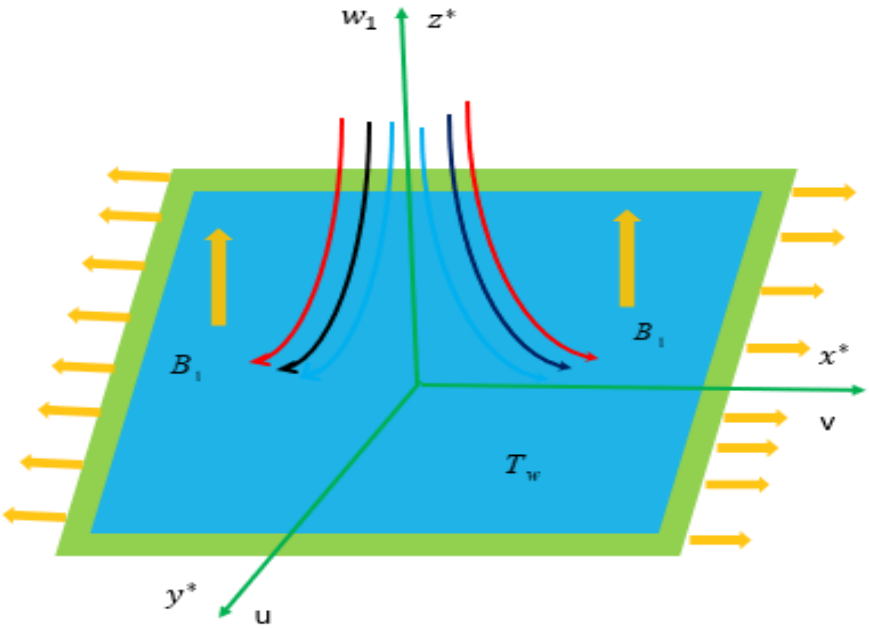

Fig. 1 Physical Geometry of the Model

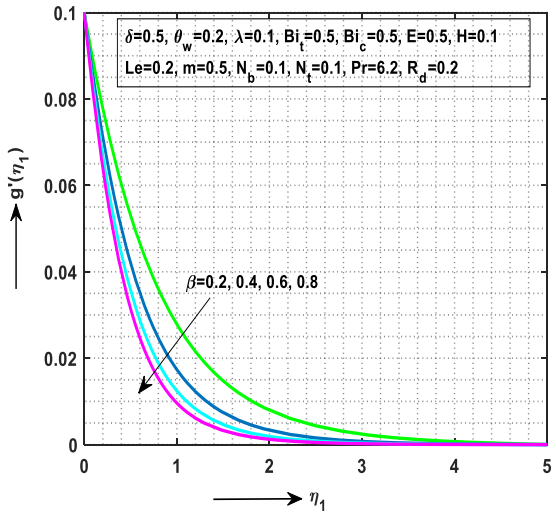

Fig. 2 Impact of β on $g'(\eta_1)$

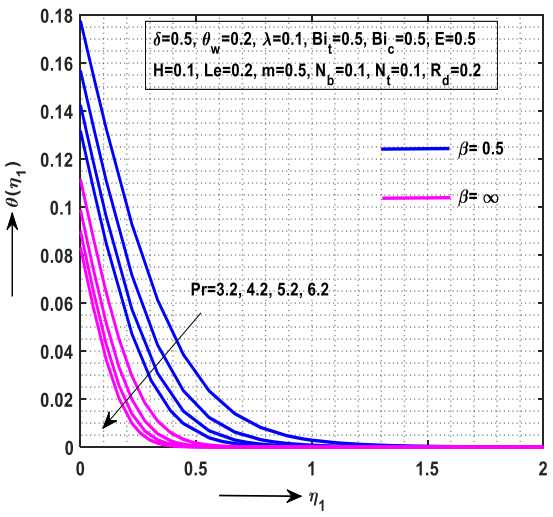

Fig. 3(a) Impact of Pr on $\theta(\eta_1)$

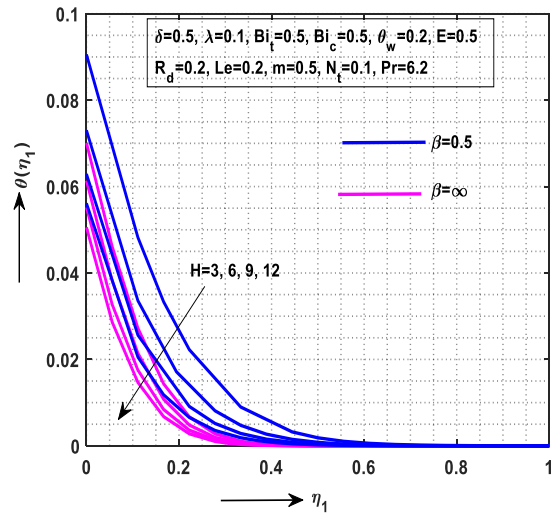

Fig. 3(b) Impact of H on $\theta(\eta_1)$

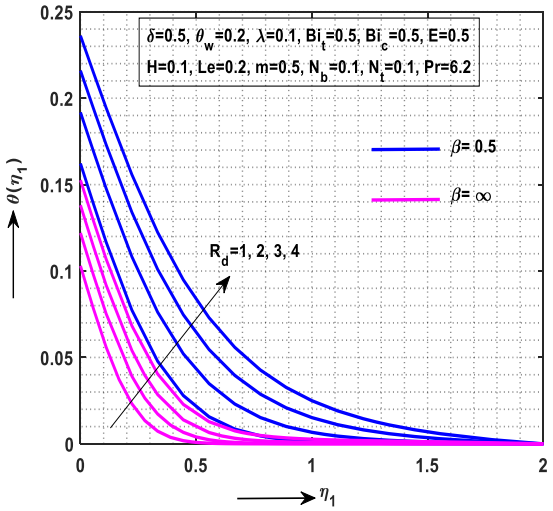

Fig. 3(c) Impact of R_d on $\theta(\eta_1)$

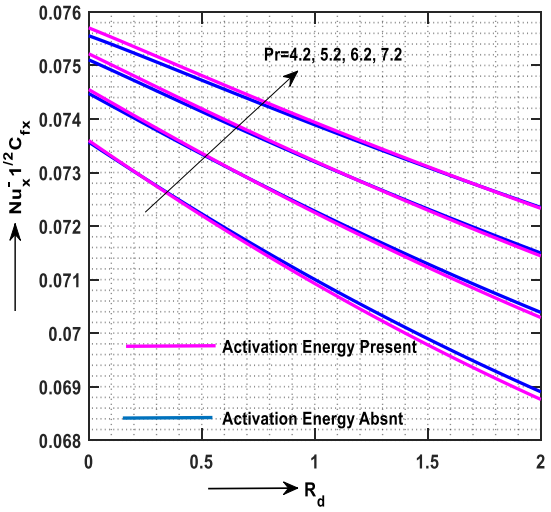

Fig. 4 Impact of Pr on $Nu_x \, \mathrm{Re}_x^{-0.5}$

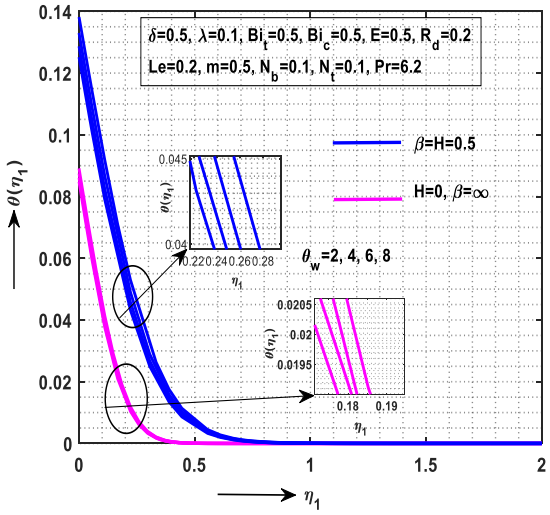

Fig. 5(a) Impact of θ_w on $\theta(\eta_1)$

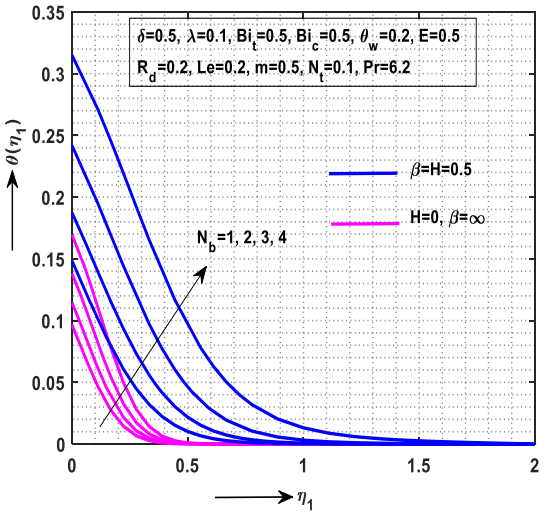

Fig. 5(b) Impact of N_b on $\theta(\eta_1)$

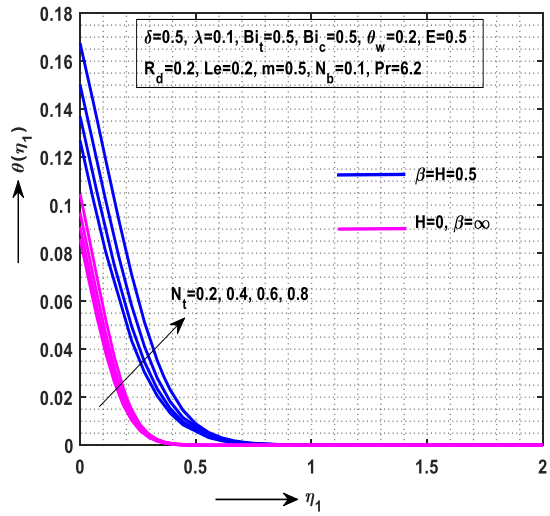

Fig. 5(c) Impact of N_t on $\theta(\eta_1)$

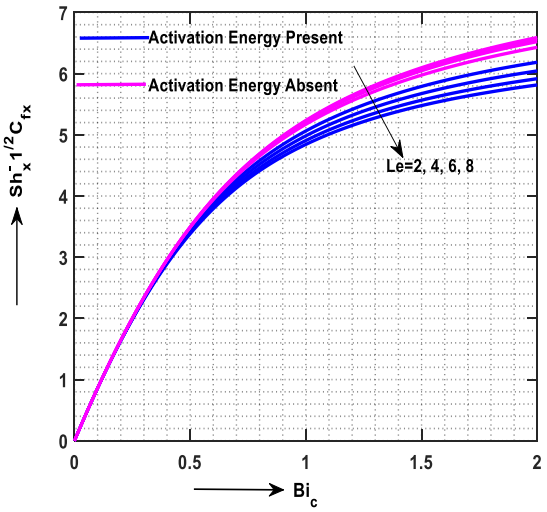

Fig. 6 Impact of Le on $Sh\,\mathrm{Re}_x^{-1.5}$

Table. 1 Evaluation of Skin friction coefficient $\left(1+\beta^{-1}\right) f''(0)$, $\left(1+\beta^{-1}\right) g''(0)$ for various values λ .

λ	**Wang [29]** $-f''(0)$	**Thammanna et al. [30]**	**Present study** $-f''(0)$	**Wang [29]** $-g''(0)$	**Thammanna et al. [30]**	**Present study** $-g''(0)$
0.00	1.000000	1.000000	1.0000000	0.000000	1.000000	0.0000000
0.20			1.0394984			0.1487378
0.25	1.048813	1.04881	1.0488134	0.194564	1.04881	0.1945649
0.40			1.0757886			0.3492102
0.50	1.093097	1.09309	1.0930971	0.465205	1.09309	0.4652066
0.60			1.1099465			0.5905307
0.75	1.134485	1.13450	1.1344852	0.794622	1.13450	0.7946279
0.80			1.1424882			0.8666843
1.00	1.173720	1.17372	1.1737212	1.173720	1.17372	1.1737209

Table. 2 Comparison of Skin friction coefficient for $\beta \to \infty$ and various values of λ

λ	**Wang [29]** $f(\infty)$	**Present study** $f(\infty)$	**Wang [29]** $g(\infty)$	**Present study** $g(\infty)$
0.00	1.000000	1.0000000	0.000000	0.0000000000
0.20		0.9226531		0.2323612
0.25	0.907075	0.9070753	0.257986	0.2579868
0.40		0.8660339		0.3792267
0.50	0.842360	0.8423606	0.451671	0.4516711
0.60		0.8209620		0.5189601
0.75	0.792308	0.7923087	0.612049	0.6121264
0.80		0.7835000		0.6414335
1.00	0.751527	0.7515275	0.751527	0.7514855